Materials Transactions, Vol. 64, No. 7 (2023) pp. 1526 to 1536
Special Issue on Superfunctional Nanomaterials by Severe Plastic Deformation

Review

Superplasticity in Severely Deformed High-Entropy Alloys

Hamed Shahmir[1,*], Mohammad Sajad Mehranpour[2], Megumi Kawasaki[3] and Terence G. Langdon[4]

[1]*Department of Materials Engineering, Tarbiat Modares University, Tehran, Iran*
[2]*School of Metallurgy and Materials, College of Engineering, University of Tehran, Tehran, Iran*
[3]*School of Mechanical, Industrial and Manufacturing Engineering, Oregon State University, Corvallis, OR, 97331, USA*
[4]*Materials Research Group, Department of Mechanical Engineering, University of Southampton, Southampton SO17 1BJ, UK*

High-entropy alloys (HEAs) are a new class of material producing superior properties that have a potential for replacing many structural materials in industry. Single-phase solid solution HEAs with face-centered cubic crystal structure show significant ductility and toughness over a wide temperature range including at cryogenic temperatures. Nevertheless, the occurrence of decomposition at elevated temperatures is challenging for many applications. These materials reveal sluggish diffusion and therefore high thermal stability so that processing by severe plastic deformation gives increased kinetics of decomposition and leads to fine-multiphase microstructures which provide a potential for achieving superior superplastic elongations. The present review is designed to examine the available superplastic data for HEAs and thereby to compare the behavior of HEAs with conventional superplastic alloys. [doi:10.2320/matertrans.MT-MF2022008]

(Received January 18, 2023; Accepted March 23, 2023; Published April 14, 2023)

Keywords: *high-entropy alloys, microstructure engineering, severe plastic deformation, superplasticity, ultrafine-grained materials*

1. Introduction

High-entropy alloys (HEAs) containing five or more principal elements (each elemental concentration between 5 and 35 at%) with a relatively simple structure have attracted much attention during the last two decades.[1–3] These alloys with high-mixing entropy promote the formation of random solid solutions with desirable properties. HEAs are very attractive materials due to their potential promising properties such as high strength, high thermal stability and oxidation resistance which offer many potential applications in various fields.[4–10] Thus, the interest of researchers has been stimulated in order to carry out research in the processing, characterization and application of HEAs. However, many experimental investigations together with thermodynamic predictions based on calculations of the phase diagrams reveal decomposition of the single-phase concentrated solid-solution phase and the formation of multi-phase microstructures containing geometrically or topologically close-packed phases such as eta and sigma phases, respectively, at elevated temperatures.[11–13] These newly-formed phases may have an intermetallic character which is generally considered to provide high strength at the expense of a significant decrease in ductility.[12–14] It was reported earlier that these materials reveal sluggish diffusion which provides high thermal stability and therefore postpones the decomposition procedure kinetically.

Severe plastic deformation (SPD) is a novel class of processing that has been used to apply a very high strain to a material without its failure and providing a capability for grain refinement to the submicrometer or nanometer scale in different materials.[15] In addition, SPD has been used to fabricate a composite with remarkable properties and cold consolidation.[15,16] Significant grain refinement together with the formation of a high density of lattice defects and unique microstructural features leads to advanced mechanical and functional properties such as a shape memory effect, hydrogen storage performance, magnetic properties, radiation resistance and corrosion resistance.[17–19] This procedure is even capable of facilitating a martensitic phase transformation in different materials including HEAs.[19–21]

Nevertheless, severe plastic deformation leads to an increased kinetic of decomposition of single-phase HEAs due to the decoration of a large number of defects such as grain boundaries which serve as fast diffusion pathways and also as preferential nucleation sites for the formation of new phases.[21–24] This provides the potential for achieving ultrafine-multiphase microstructures under controlled post-deformation heating where this is capable of exhibiting superplastic elongations (>400%) in a number of HEAs.[25,26]

Even after almost twenty years since the introduction of HEAs, it is now only the beginning for developing a fundamental understanding of these materials from the point of view of interpreting the relationship between the microstructures and the mechanical properties at elevated temperatures. Accordingly, this review was undertaken to provide a summary of the main attempts undertaken to date to achieve superplasticity in these alloys and therefore to make a systematic comparison with conventional engineering materials and to clarify the advantages and high potential of HEAs for industrial applications.

2. Basic Superplastic Flow Behavior and the Significance of Severe Plastic Deformation

Superplasticity refers to the exceptionally high strains which may be achieved in alloys before failure when pulling in tension under a constant rate of straining. In order to provide a definitive criterion for the occurrence of superplastic flow, the advent of superplasticity is now defined as a measured tensile elongation of at least 400%.[26] This behaviour is an important feature of alloys that are used for industrial superplastic forming operations where complex curved shapes are fabricated for use in a range of applications.[27] It is well established that there are two

*Corresponding author, E-mail: shahmir@modares.ac.ir

essential requirements for attaining superplasticity including a very small grain size (typically $<10\,\mu m$) and conducting the operation at relatively high temperatures of at least $\sim 0.5T_m$ which T_m is the absolute melting temperature.[28] Basically, superplastic flow is a diffusion-controlled process which becomes important at elevated temperatures.

It is important to note that in industry these very small grains are typically achieved through thermo-mechanical treatments which are capable of reducing the grain sizes to ~2–5 μm. Nevertheless, over the last three decades it has become clear that even smaller grains, typically within the submicrometer or even the nanometer range, may be attained by processing metals and alloys through the application of severe plastic deformation (SPD).[29–33] Accordingly, SPD was demonstrated as a new processing procedure having a great potential for achieving ultrafine-grained materials and therefore providing superplasticity during subsequent plastic deformation[34] and this approach is now used extensively for achieving excellent superplastic forming capabilities.[35] Although there are several different SPD processing techniques, most attention to date has focussed on the two different procedures of equal-channel angular pressing (ECAP)[36] where a rod or bar is pressed through a special die containing a channel bent through a sharp angle and high-pressure torsion (HPT)[37] where a disk is subjected to high applied pressure and concurrent torsional straining.

There is a definitive criterion for the occurrence of superplastic flow in which the measured tensile elongation should be at least 400% with a strain rate sensitivity of $m \approx 0.5$.[26,38] It has been demonstrated that the main mechanism in superplastic flow is the occurrence of grain boundary sliding (GBS)[39] and this sliding must be accommodated by the glide of intragranular dislocations that cross the grains, pile up at the opposite grain boundaries and then climb into the boundaries.[40,41] A theoretical model based on grain boundary sliding leads to a superplastic strain rate, $\dot{\varepsilon}_{sp}$, which is given by the following general power-law relationship:[42]

$$\dot{\varepsilon}_{sp} = \frac{A D_{gb} G \mathbf{b}}{kT} \left(\frac{\mathbf{b}}{d}\right)^2 \left(\frac{\sigma}{G}\right)^2 \quad (1)$$

where A is a dimensionless constant having a value of ~10, D_{gb} is the coefficient for grain boundary diffusion, G is the shear modulus, **b** is the Burgers vector, k is Boltzmann's constant, T is the absolute temperature, d is the grain size and σ is the applied stress. Based on the importance of GBS as the deformation mechanism in superplastic flow, grain refinement is the key to extending the superplastic regime into a wider stress region at faster strain rates. In addition, grain refinement after processing through SPD leads to an increase in the volume fraction of high-angle grain boundaries and this contributes to the sliding activity.[43] Equation (1) provides an excellent description of the superplastic flow of both conventional metals with grain sizes of a few micrometers as well as ultra-fine grained alloys processed by SPD followed by heating to elevated temperatures.[44] Specifically, it was shown that there is very good agreement between published data and the predictions of eq. (1) for many conventional materials including Al-based and Mg-based alloys.[45–47]

In practice, performing tensile testing at elevated temperatures significantly affects the microstructure by facilitating the driving force required for microstructural coarsening and this may significantly reduce the ductility at temperatures where superplasticity is expected. Accordingly, having two phases or even a multi-phase structure is an important requirement for maintaining a fine-grained microstructure in which these separate phases lead to a significant inhibition of grain growth in materials containing a fine dispersion of a second phase to act as a grain refiner. The potential for using HEAs for the formation of stable multiphase microstructures at relatively high temperatures provides remarkable advantages for achieving significant superplasticity in these alloys. Accordingly, it is important to evaluate whether the same agreement between the theoretical model for superplasticity and the experimental data applies also to the occurrence of superplastic flow in HEAs.

3. The Role of the High-Entropy Alloy Characteristics in Superplasticity

To achieve significant superplastic properties, the alloy must have, or at least must develop, high thermal stability and significant grain growth resistance by suppressing grain boundary migration.[38] It is important to note that the formation of second phases in conventional alloys to retain a grain size to the range of lower than 10 μm is known as an essential factor for superplasticity. Nevertheless, low thermal stability of conventional alloys and coarsening of grain and precipitates are responsible for a deterioration of superplasticity in these materials.

The inherent sluggish diffusion together with the provision of strong obstacles to limit grain boundary mobility are key factors in improving the thermal stability at elevated temperatures. The results presented in Fig. 1(a) show that the value of the activation energy for the diffusion of different elements in the well-studied CoCrFeNiMn HEA is much higher by comparison with other conventional alloys and this leads to sluggish diffusion.[22,48] In addition, Fig. 1(b) shows the activation energy for grain growth in different alloys which demonstrates directly the greater difficulty of achieving grain growth in the HEA.[49–54] In practice, it was established that grain boundary diffusion of an element having the lowest diffusion coefficient (Ni in the CoCrFeNiMn HEAs) controls the rate of flow in superplasticity.[22,48] Basically, solid solution strengthening in HEAs depends on the chemical bonding and the size mismatch of the various components. Accordingly, there is a significant potential that boundary mobility is controlled by solute atoms in HEAs although solute drag will become less effective at high temperatures. It was reported that coarsening in the CoCrFeNiMn HEA exhibits a classical power-law behaviour with an exponent of 3 which suggests that the grain boundary motion is controlled by a solute-drag mechanism when the material is in a single-phase condition.[55–58]

In addition, any precipitates appearing in the microstructure during exposure to heat are found to be especially effective in pinning the grain boundaries. In practice, these precipitates restrict dislocation motion and therefore inhibit the movement of grain boundaries so that consequently they

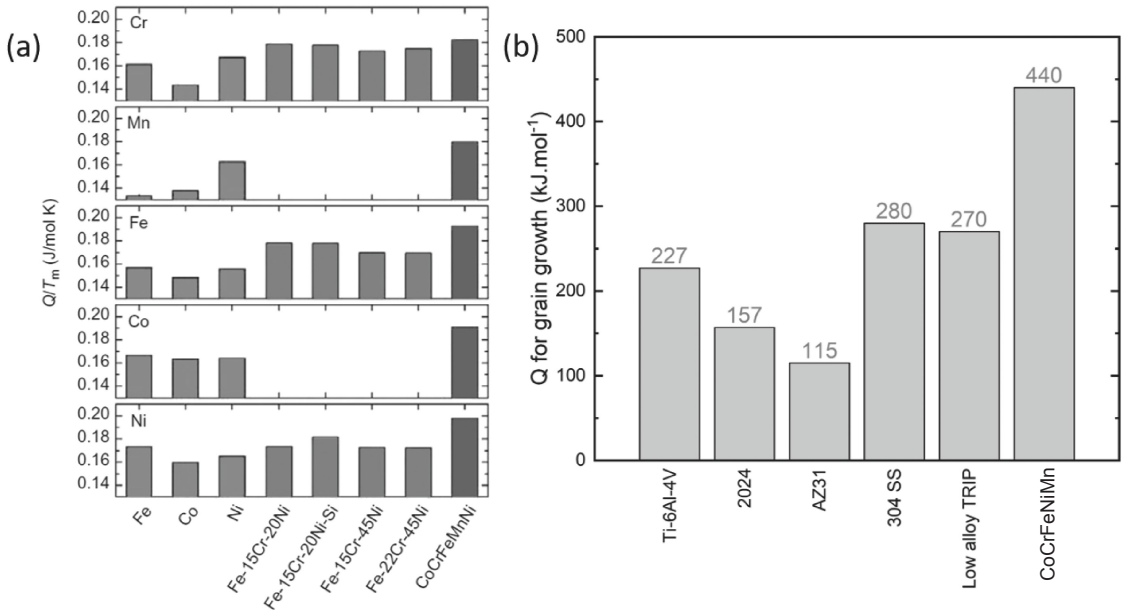

Fig. 1 (a) Activation energy of diffusion for different elements[48] and (b) activation energy of grain growth for different alloys (data based on Refs. 49)–54)) in different metals and alloys.

decelerate the occurrence of microstructural coarsening.[59] Clearly, the size and the volume fraction of these precipitates depend on the annealing temperature which consequently affects the pinning force in the Zener effect and the grain sizes.[60,61] It was reported in many investigations on conventional alloys that remarkable superplasticity is related to the presence of second phases which are effective in preventing grain growth by the Zener pinning mechanism. Accordingly, it is expected that any second phase will improve the occurrence of superplasticity in the HEAs. Actually, there is an intrinsic potential of decomposition and formation of second phases in HEAs at elevated temperatures encouraged by SPD. High defects in the microstructure generated during SPD provide fast diffusion pathways and a high volume fraction of interfaces as preferential nucleation sites promotes the formation of new phases. This provides the potential for achieving ultrafine-multiphase microstructures under a controlled hot deformation regime which is capable of exhibiting superplasticity in HEAs. There are many precipitates in HEAs such as sigma or NiAl-B2 and these can improve the superplastic properties (see Fig. 2).[62,63] Accordingly, it is concluded that HEA alloys have unique characteristics of intrinsic resistance to grain boundary mobility and high thermal stability by comparison with conventinal alloys which lead to significant superplastic properties.

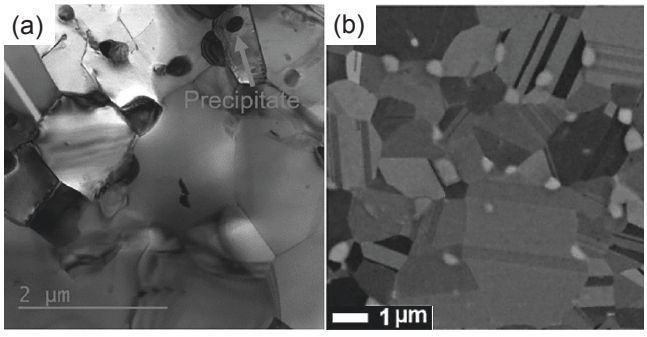

Fig. 2 (a) Bright-field TEM image of $CoCrFeNiMnTi_{0.1}$[81] and (b) SEM-BSE image of $V_{10}Cr_{15}Mn_5Fe_{35}Co_{10}Ni_{25}$[91] HEAs after post-deformation annealing at 800°C for 60 min.

4. Evidence of Superplastic Flow in HEAs and the Importance of a Secondary Phase

The first evidence of superplasticity in HEAs was reported in a fine multiphase equiaxed structure of an AlCoCrCuFeNi alloy with an average grain/particle size of ~2 μm processed through multidirectional hot forging at 950°C.[64,65] The microstructures represented in Fig. 3 denote multiphase structures including (i) a Cu-rich phase with an ordered *fcc* structure, (ii) an Al–Ni-rich phase with an ordered B2 structure, (iii) a Cr–Fe-rich phase with a disordered *bcc* structure and (iv) a Co–Cr–Fe-rich phase with an ordered *fcc* structure. It was reported that processing by SPD changed the ordering of the Cu-rich and Co–Cr–Fe-rich phases and led to a transformation of the *bcc* Cr–Fe-rich phase to a sigma phase with a topologically close-packed structure.[64,65] Figure 3(c) shows the values of the total elongations in the temperature range of room temperature up to 1000°C at a strain rate of $10^{-3}\,s^{-1}$ in two conditions before and after SPD which clearly shows the advantage of applying SPD.[64,65] The results indicate a significant increase in elongation by increasing the temperature from 700 to 800°C due to a brittle to ductile transition in which the grain refinement from hot forging reduces this transition temperature by ~100°C compared to the as-cast condition.[65] The significant increase in ductility at >700°C is mainly due to the activation of mechanisms related to grain boundaries such as GBS accommodated by diffusion-controlled processes. The strain rate sensitivity index or m value was in the range of ~0.37–0.56 which is consistent with the value of $m \approx 0.5$ which is associated with fine-grained superplasticity when GBS is the rate-controlling deformation mechanism.[64] Figure 3(d)

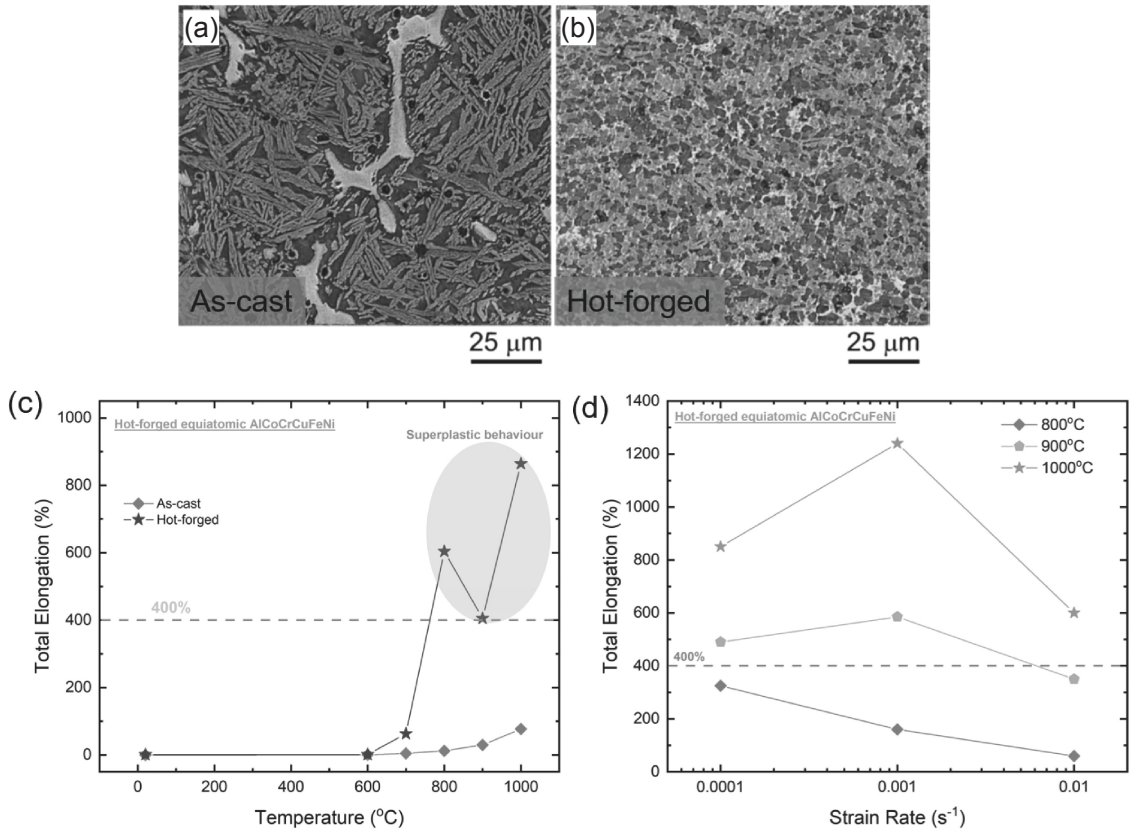

Fig. 3 Microstructures of AlCoCrCuFeNi HEA in (a) as-cast[65] and after (b) multidirectional hot forging at 950°C. (c), (d) A summary of the tensile elongations under different conditions[64,65] where the horizontal dashed line at 400% represents the critical criterion for achieving true superplastic behaviour.

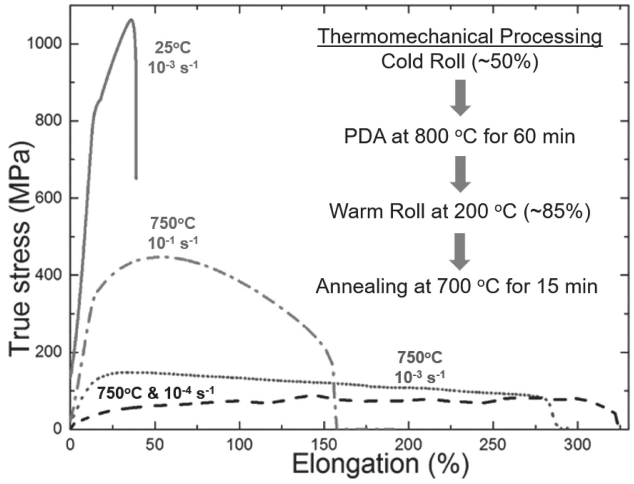

Fig. 4 True stress-elongation (%) curves of a fine-grained CoCrFeNiMn HEA at room temperature and 750°C for different strain rates.[67]

shows the effect of the strain rate on the superplastic flow in which a strain rate of $10^{-3}\,s^{-1}$ reveals the maximum total elongations at various temperatures.[64] This alloy shows significant resistance to grain growth which may be due to the complex microstructure and the presence of various precipitates.[64,66]

Figure 4 shows the results of a study of the high-temperature mechanical properties of an equiatomic CoCrFeNiMn HEA after processing by a complex thermo-mechanical treatment including cold rolling with a reduction in thickness of ~50%, post-deformation annealing at 800°C for 1 h, warm rolling at 200°C with a reduction in thickness of ~85% and finally annealing at 700°C for 15 min.[67] The final microstructure contained single-phase *fcc* with a grain size of ~1.4 μm. The results show that increasing the temperature from room temperature to 750°C reduces the flow stress and dramatically increases the ductility. However, superplasticity was not achieved because all elongations were <400% and it was suggested that increasing the extent of grain refinement may lead to superplasticity.[67]

In a later investigation,[68] significant grain refinement was attained using HPT in a CoCrFeNiMn HEA where HPT processing was adopted as one of the commonly used SPD methods for applying heavy strains to alloys in order to improve the superplastic properties.[21,36,37,53,69,70] The results are shown in Fig. 5(a) and they depict a single-phase microstructure with an average grain size of <100 nm after HPT processing. The high-temperature mechanical properties of the nano-grained material revealed superplasticity with a maximum total elongation of ~620% at 973 K under a strain rate of $10^{-3}\,s^{-1}$ (Fig. 5(b)). It was suggested that the formation of precipitates in the temperature range of 600 to 800°C plays an important role in maintaining the fine microstructure at high temperatures and therefore improving the superplastic flow (Fig. 5(c)).[68] Numerous studies have been carried out on precipitation in the CoCrFeNiMn HEA and the results show that *bcc* and sigma Cr-rich precipitates are formed in the temperature range between 600 and 800°C and these precipitates start to dissolve above 750°C.[23,71–74]

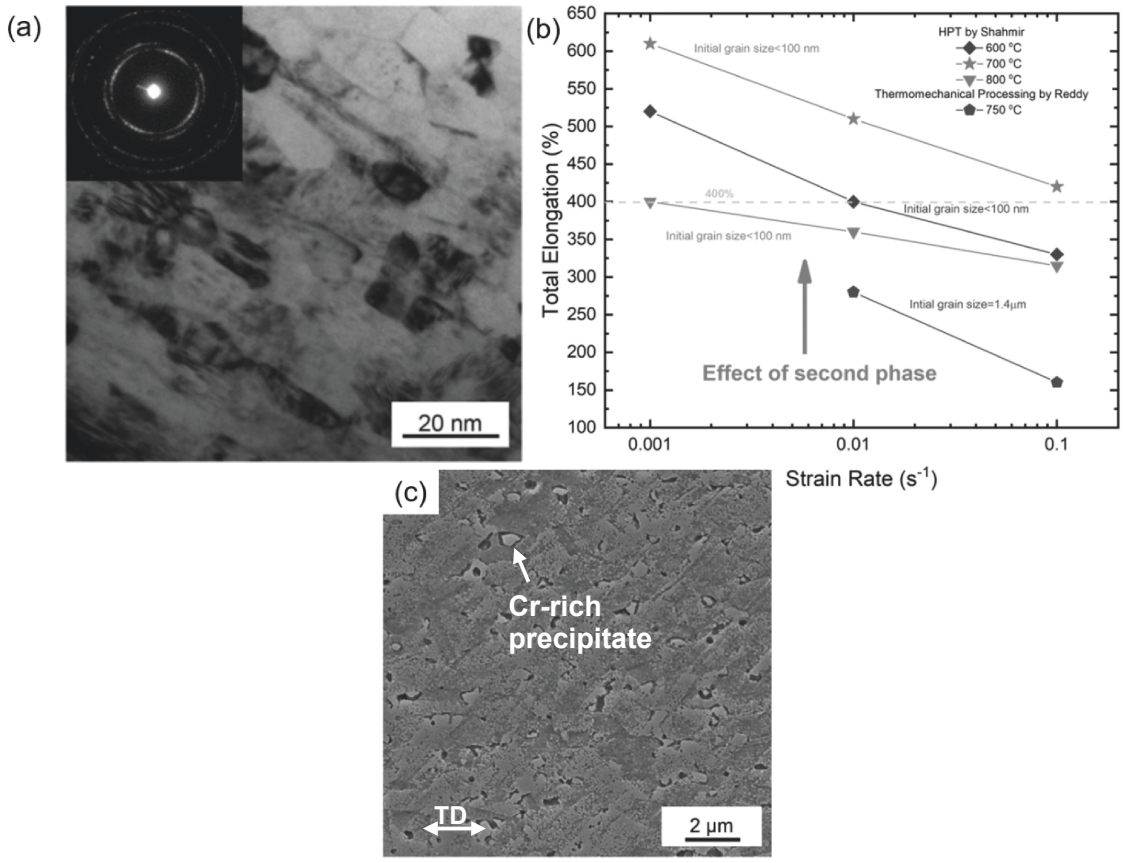

Fig. 5 (a) Microstructure of the CoCrFeNiMn HEA after HPT processing,[68] (b) total elongation versus strain rate for different conditions[67,68] and (c) microstructure after tensile testing at 700°C[68] where TD is the tensile direction.

The origin for the formation of new phases in the nanocrystalline CoCrFeNiMn HEA is due to the large number of grain boundaries which serve both as fast diffusion pathways and also as preferential nucleation sites for the formation of new phases.[74–76] Thus, these precipitates place many strong obstacles in the path of grain growth for the CoCrFeNiMn HEA and their dissolution at >750°C produces a significant drop in the superplastic behavior due to rapid grain growth and the formation of microcracks under loading at these elevated temperatures.[68]

Ti[77] and Al[78–80] elements were added to CoCrFeNiMn HEA in order to increase the volume fraction of precipitates and also increase their stability by using microstructure engineering and therefore to improve the superplastic behavior of the fabricated HEAs. Figure 6 provides a summary of the superplastic properties of CoCrFeNiMn HEAs after the addition of minor amounts of Al and Ti. The results suggest that the presence of these elements leads to a significant improvement in the superplastic behavior of CoCrFeNiMn with elongations of >800% and >1200% for alloys containing Ti and Al, respectively. This is attributed to the creation of stable obstacles against grain growth. It was reported that introducing a small fraction of hard phases such as B2-NiAl can dramatically restrain the occurrence of dynamic grain growth.[80]

It was shown that the Ti addition to the HEA promotes the formation of Cr-rich precipitates, increases the stability of these precipitates and increases the stability of the grains up to higher temperatures than 800°C (see Fig. 7).[72,77,81] The

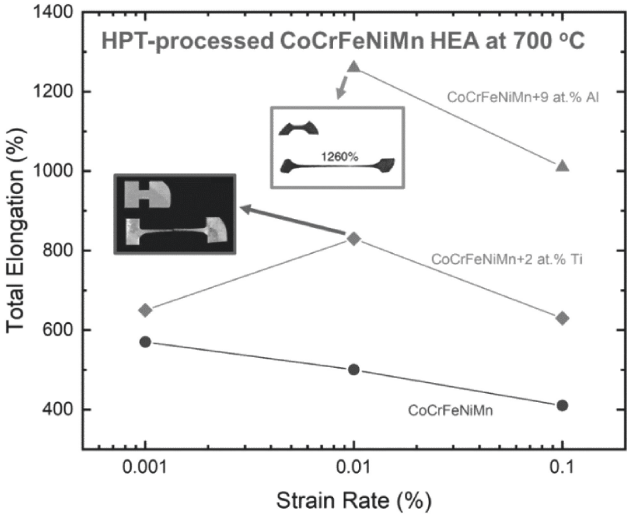

Fig. 6 Elongation diagrams of HPT-processed CoCrFeNiMn, $CoCrFeNiMnTi_{0.1}$ and $CoCrFeNiMnAl_{0.5}$ HEAs after testing at 700°C (data based on Refs. 68), 77), 78)).

microstructure of a CoCrFeNiMn+9 at% Al after HPT processing contained equiaxed grains of an *fcc* phase with an average grain size of ~2 μm together with fine NiAl-B2 precipitates (~0.8–1 μm) formed at grain boundaries in the matrix and ultrafine NiAl-B2 precipitates (~200–400 nm) within the grains.[78] The formation of NiAl-B2 precipitates was related to the high negative mixing enthalpy (−22.3 kJ mol^{-1}) between Ni and Al and the large atomic size of Al

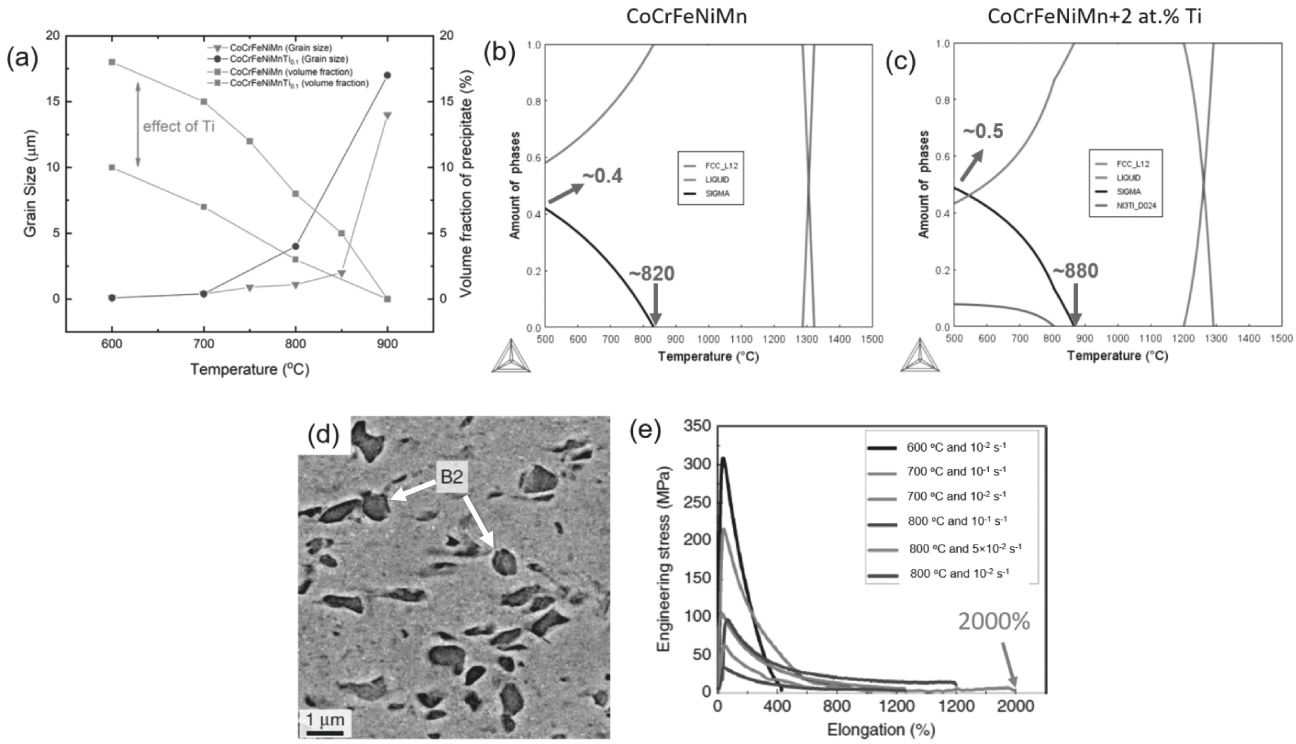

Fig. 7 (a) Effect of Ti addition on the microstructure of the CoCrFeNiMn alloy at elevated temperatures.[68,77] (b) and (c) Thermo-Calc diagrams of CoCrFeNiMn HEA[81] and CoCrFeNiMn+2 at% Ti HEAs,[81] respectively. (d) Backscattered Electron image of the HPT-processed CoCrFeNiMn+9 at% Al[78] and (e) engineering stress versus elongation for HPT-processed CoCrFeNiMn+9 at% Al after testing at elevated temperatures.[78]

by comparison with other elements which promotes the formation of a bcc phase. Figure 7(d) demonstrates the microstructure of the CoCrFeNiMn+9 at% Al HEA after HPT processing and shows the existence of the B2 phase in the severely deformed microstructure without any significant reduction in size.[78] An extraordinary superplastic flow for the Al-added senary HEA, represented in Fig. 7(e), shows an elongation to failure of up to 2000% under a strain rate of $5 \times 10^{-2}\,s^{-1}$ at 800°C.[78] It was reported in another investigation that grain refinement of a $CoCrFeNiMnAl_{0.5}$ HEA due to thermomechanical treatment led to improved superplastic properties at 1000°C by comparison with the quinary HEA due to higher thermal stability of the fine-grained microstructure in the senary HEA.[79]

There are some studies which suggest the importance of other precipitates in fine and ultrafine-grained microstructures including sigma phase formation to pin the grain boundaries at elevated temperatures and to thereby improve the superplastic properties of HEAs. It is important to note that this brittle phase reduces the mechanical properties of these alloys at lower temperatures. A non-equiatomic $V_{10}Cr_{15}Mn_5Fe_{35}Co_{10}Ni_{25}$ HEA was developed[82] and the mechanical properties were compared at elevated temperatures with the CoCrFeNiMn HEA. The results revealed an improvement in superplastic properties due to the formation of sigma Cr-rich precipitates as obstacles against grain growth. A maximum elongation of 770% was reported during tensile testing at 700°C under a strain rate of $3.3 \times 10^{-3}\,s^{-1}$. It was concluded that the presence of the V element encourages the formation of this secondary phase in the senary HEA.[82]

Another study was conducted on an $Fe_{42}Mn_{28}Co_{10}Cr_{15}Si_5$ dual-phase HEA with an average grain size of ~0.7 μm processed by friction-stir processing.[83] This material contained a high-volume fraction (42%) of sigma precipitates and showed an elongation to failure of 550% under a strain rate of $10^{-3}\,s^{-1}$ at 700°C. Significant Cr partitioning occurred at 700°C and was responsible for sigma formation. Also, reducing the strain rate during testing led to a significant increase in sigma precipitation.[83] Another study was conducted on the superplastic properties of an HPT-processed $Mo_{7.5}Fe_{55}Co_{18}Cr_{12.5}Ni_7$ alloy at 700 and 800°C.[84] This investigation showed a complex multiphase microstructure including *fcc*, *bcc* martensite and Mo-rich μ phase (see Fig. 8(a)) before tensile testing at high temperatures. The results in Fig. 8(b) illustrate an elongation to failure of >400% at 800°C but no superplasticity was observed during testing at 700°C. This was related to the formation of more Mo-rich μ precipitates at higher temperatures.[84]

For the HPT-processed $CoCrNiAl_{0.3}$ alloy, it was suggested that partial melting of Al segregation at the grain boundaries together with the formation of sigma and B2 precipitates led to significant superplasticity including a total elongation of ~1200% under a strain rate of $5 \times 10^{-2}\,s^{-1}$ at 800°C (see Fig. 9).[85] By making a comparison between the HPT-processed $CoCrNiAl_{0.3}$ and $CoCrFeNiMnAl_{0.5}$ samples, it is apparent that increasing the volume fraction and decreasing the size of the sigma and B2 precipitates improves the high strain rate superplastic properties of these alloys by hindering the grain growth process (see Fig. 10). It was reported that the slightly better properties of $CoCrNiAl_{0.3}$ after post-deformation annealing (PDA) at 800°C compared to

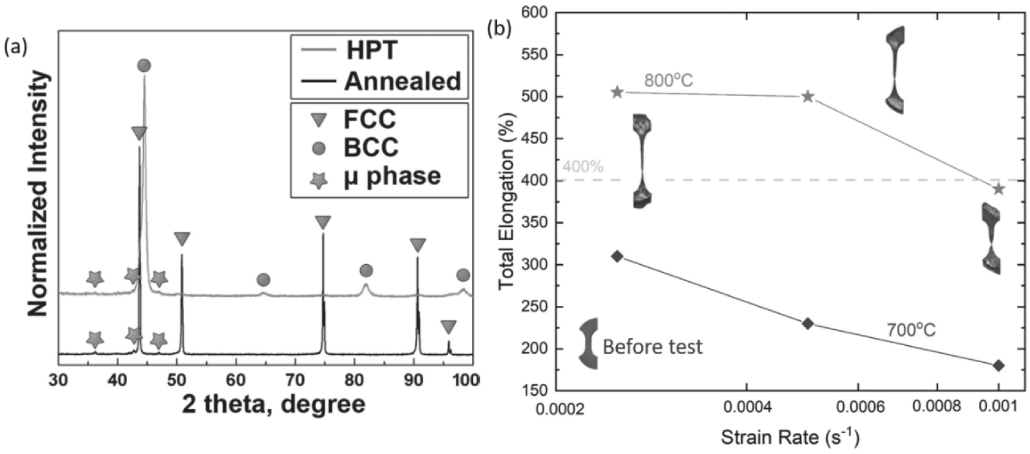

Fig. 8 (a) XRD patterns of $Mo_{7.5}Fe_{55}Co_{18}Cr_{12.5}Ni_7$ HEA before (annealed) and after HPT processing and (b) elongation-strain rate diagram of HPT-processed samples before and after testing at elevated temperatures.[84)]

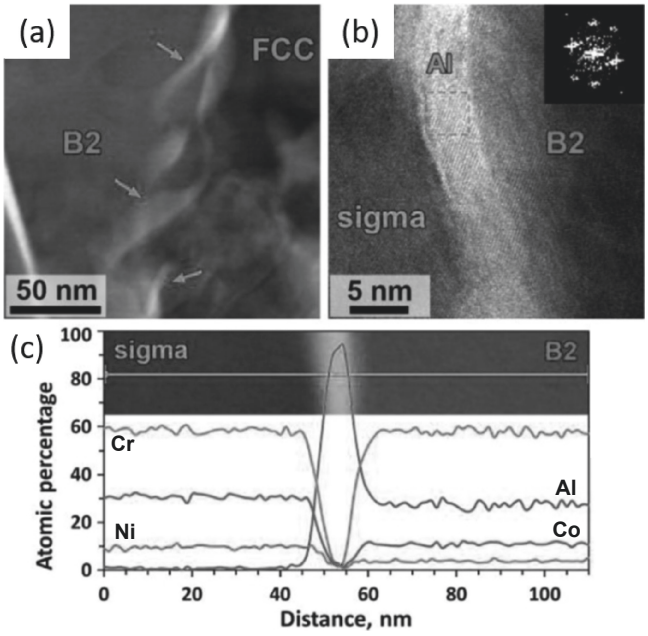

Fig. 9 (a) STEM image of deformation-induced grain boundary segregation in $CoCrNiAl_{0.3}$, (b) HRTEM image of deformation-induced grain boundary segregation in $CoCrNiAl_{0.3}$ and (c) the EDS line-scan through sigma and B2 grains.[85)]

annealing at 900°C was due to a smaller sigma phase in the former alloy (~300 vs. ~380 nm). It appears that larger sigma particles promote cavitation through local stress concentrations that are generated around the grains and this reduces the superplasticity.[86)]

5. Analysis of the Flow Mechanism in Superplastic HEAs

There are some limited results now available documenting the occurrence of superplasticity in several HEAs and these data are summarized in Table 1. The present information provides the key parameters including the composition of the HEA, the processing procedure used to attain a superplastic grain size, the gauge dimensions of the tensile specimens, the temperature and strain rate of the tensile testing and the measured elongations to failure. As noted earlier, superplasticity is defined formally as a tensile elongation of at least 400% and therefore some of these results are strictly outside of the range required for true superplastic flow and therefore they represent "superplastic-like flow" with additional evidence that the ductility may be limited due to the concomitant occurrence of cavitation.[67)] Accordingly, there are some promising available results on fine and ultra-grained HEAs, particularly alloys containing Al, which indicate

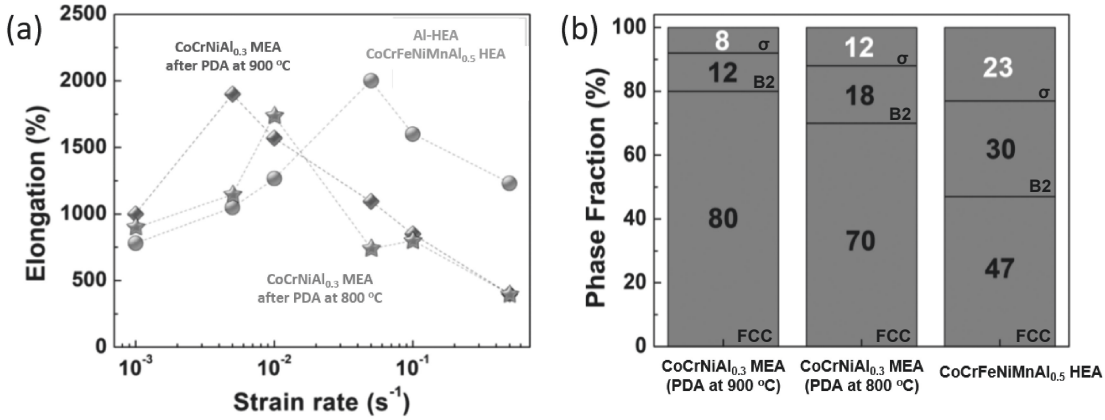

Fig. 10 (a) Elongation-strain rate diagram of HPT-processed $Al_{0.3}CoCrNi$ and $Al_{0.5}CoCrFeNiMn$ samples and (b) volume fraction of all phases in $CoCrNiAl_{0.3}$ and $CoCrFeNiMnAl_{0.5}$ alloys.[86)]

Table 1 Experimental results for superplasticity and superplastic-like flow in high-entropy alloys.

Composition	Processing	Gauge dimensions (mm^3)	Temp. (°C)	Strain rate (s^{-1})	El. (%)	Reference
AlCoCrCuFeNi	Multiaxial forging	16 × 3 × 1.5	800	1.0×10^{-3}	160	Shaysultanov *et al.* [64] and Stepanov *et al.* [66]
			800	1.0×10^{-4}	325	
			900	1.0×10^{-2}	350	
			900	1.0×10^{-3}	585	
			900	1.0×10^{-4}	490	
			1000	1.0×10^{-1}	600	
			1000	1.0×10^{-2}	1240	
			1000	1.0×10^{-3}	850	
AlCoCrCuFeNi	Multiaxial forging	16 × 3 × 1.5	800	1.0×10^{-3}	604	Kuznetsov *et al.* [90]
			900	1.0×10^{-3}	405	
			1000	1.0×10^{-1}	442	
			1000	1.0×10^{-2}	858	
			1000	1.0×10^{-3}	864	
			1000	1.0×10^{-4}	753	
CoCrFeNiMn	HPT	1.1 × 1.0 × 0.6	500	1.0×10^{-3}	160	Shahmir *et al.* [68]
			600	1.0×10^{-1}	330	
			600	1.0×10^{-2}	400	
			600	1.0×10^{-3}	520	
			700	1.0×10^{-1}	410	
			700	1.0×10^{-2}	500	
			700	1.0×10^{-3}	570	
			800	1.0×10^{-1}	310	
			800	1.0×10^{-2}	360	
			800	1.0×10^{-3}	390	
$CoCrFeNiMnTi_{0.1}$	HPT	1.1 × 1.0 × 0.6	600	1.0×10^{-2}	460	Shahmir *et al.* [77]
			700	1.0×10^{-1}	630	
			700	1.0×10^{-2}	830	
			700	1.0×10^{-3}	650	
			800	1.0×10^{-2}	570	
$CoCrFeNiMnAl_{0.5}$	HPT	1.5 × 1.0 × 0.7	600	5.0×10^{-1}	250	Nguyen *et al.* [78]
			600	1.0×10^{-2}	430	
			700	5.0×10^{-1}	750	
			700	1.0×10^{-1}	1030	
			700	1.0×10^{-2}	1260	
			800	5.0×10^{-1}	1230	
			800	1.0×10^{-1}	1600	
			800	5.0×10^{-2}	2000	
			800	1.0×10^{-2}	1265	
			800	5.0×10^{-3}	780	
			800	1.0×10^{-3}	780	
$CoCrFeNiMnAl_{0.5}$	Thermo-mechanical processing	-	1000	1.0×10^{-1}	108	Jeong *et al.* [79]
				5.0×10^{-2}	146	
				1.0×10^{-2}	251	
				5.0×10^{-3}	309	
				1.0×10^{-3}	330	
				5.0×10^{-4}	290	
$CoCrNiAl_{0.3}$	HPT	1.5 × 1.0 × 0.7	800	5.0×10^{-1}	~400	Asghari-rad *et al.* [85]
				1.0×10^{-1}	~840	
				5.0×10^{-2}	~1180	
				1.0×10^{-2}	~1170	
				5.0×10^{-3}	~1180	
				1.0×10^{-3}	~970	
$V_{10}Cr_{15}Mn_5Fe_{35}Co_{10}Ni_{25}$	HPT	1.5 × 1.0 × 0.7	600	1.0×10^{-2}	130	Nguyen *et al.* [82]
			600	5.0×10^{-3}	225	
			600	1.0×10^{-3}	325	
			600	5.0×10^{-4}	390	
			700	1.0×10^{-2}	490	
			700	5.0×10^{-3}	480	
			700	3.3×10^{-3}	770	
			700	1.0×10^{-3}	650	
			700	5.0×10^{-4}	410	
			800	5.0×10^{-3}	580	
			800	3.3×10^{-3}	580	
			800	1.0×10^{-3}	700	
			800	5.0×10^{-4}	630	
			800	5.0×10^{-3}	615	
CoCrFeNiMn	Rolling	3 × 1 × 0.3	750	1.0×10^{-1}	160	Reddy *et al.* [67]
			750	1.0×10^{-3}	290	
			750	1.0×10^{-4}	320	
$Mo_{7.5}Fe_{55}Co_{18}Cr_{12.5}Ni_7$	HPT	1.5 × 1.0 × 0.7	800	1.0×10^{-3}	390	Nguyen *et al.* [84]
			800	5.0×10^{-4}	500	
			800	2.5×10^{-4}	505	

significant superplasticity with tensile elongations much higher than 400% and even up to ~2000%.[67] Examples of true superplasticity are shown by the samples visible in Figs. 6 and 8 where, as required by superplastic flow,[87] there is no evidence for the occurrence of any necking within the gauge lengths.

It is well-established that, in addition to an elongation of at least 400%, there is another definitive criterion for the occurrence of superplastic flow and that is a measured strain rate sensitivity of $m \approx 0.5$.[26,38] Basically, as represented in eq. (1), the theoretical model based on GBS leads to a superplastic strain rate with a power-law relationship in which the stress exponent of σ/G is equal to 2 and m corresponds to the inverse of the stress exponent so that the anticipated strain rate sensitivity is $m = 0.5$.[42] However, the measured value for m for severely deformed HEAs, as given by the slope of a plot of flow stress against the initial strain rate, typically gives an average strain rate sensitivity of $m \approx 0.3$.[68] This value is not consistent with eq. (1) although there was microstructural evidence for the occurrence of GBS in these investigations of the HEAs. Instead, a value of $m \approx 0.3$ suggests that deformation at an elevated temperature is controlled by an intragranular dislocation glide process[88] but, on the contrary, samples deforming by dislocation glide are not capable of achieving elongations as high as >400%. Accordingly, the data were interpreted in a different way by noting that an anomalously low strain rate sensitivity may be attained due to the occurrence of massive grain growth during heating where the grains in the severely deformed single-phase HEAs grew from a few tens of nanometres to a few microns before the formation of precipitates during the heating.[68] This explanation is illustrated schematically in Fig. 11. It is important to note that a higher strain rate sensitivity of $m \approx 0.4$ was reported in the HEAs[68] containing a secondary phase in the initial severely deformed microstructures before heating and testing and this may hinder the occurrence of massive grain growth during heating which

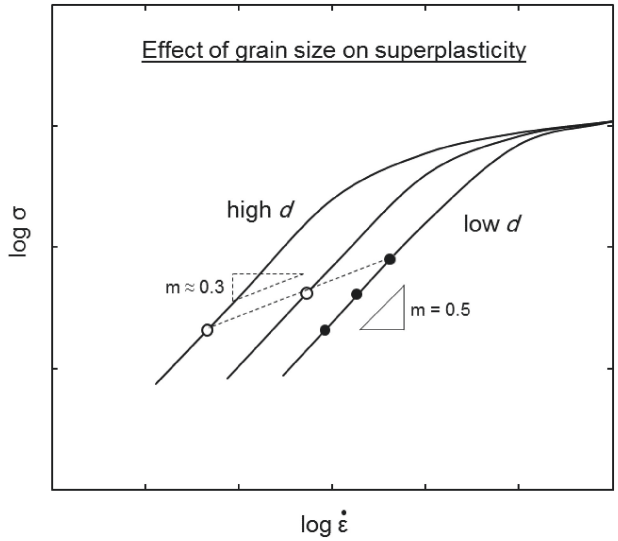

Fig. 11 Schematic illustration of stress versus strain rate showing the effect of grain refinement on an enhancement of the superplastic region at intermediate strain rates and the displacement to faster strain rates that effectively reduces the measured value of m.[68]

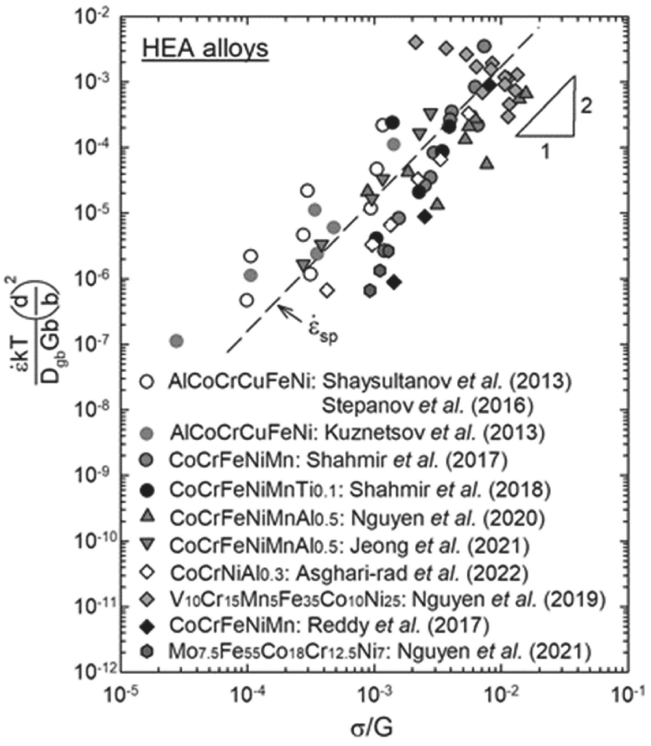

Fig. 12 Temperature and grain size compensated strain rate versus normalized stress showing excellent agreement with the theoretical prediction for conventional superplasticity.[64]

means that the HEAs then become more similar to conventional superplastic alloys.

It was already noted that eq. (1) provides an excellent description of the superplastic flow of fine and ultrafine-grained conventional materials[45–47] and accordingly it is important to check the agreement between the published data summarized in Table 1 and the prediction of the theoretical model. To evaluate the flow mechanism in the superplastic HEAs, eq. (1) was re-arranged and experimental data from each investigation were plotted in the form of the temperature and grain size compensated strain rate against the normalized stress. The results are shown in Fig. 12 with $D_{gb} = D_o \exp(-Q_{gb}/RT)$ where D_o is a frequency factor ($19.4 \times 10^{-4}\,m^2\,s^{-1}$ for pure Ni), Q_{gb} is the activation energy for grain boundary diffusion ($113\,kJ\,mol^{-1}$ for superplastic deformation of an ultrafine-grained HEA[68]), R is the gas constant, $\mathbf{b} = 2.55 \times 10^{-10}\,m$[56] and $G = 85 - \{16/(\exp(448/T) - 1)\}$ GPa.[89] The plot was constructed taking grain sizes of $d = 2.1\,\mu m$,[64,66] $1.5\,\mu m$,[90] $1.0\,\mu m$,[68] 0.5–$3.0\,\mu m$[77] and $1.4\,\mu m$.[67] The solid line labeled $\dot{\varepsilon}_{sp}$ has a slope of 2 and there is generally an excellent agreement between the experimental datum points and the theoretically predicted rate for superplasticity occurring by GBS.[42] This plot confirms that the behaviour of HEAs is generally similar to conventional alloys processed by SPD despite the well-defined characteristic differences in this new class of materials.

6. Summary and Conclusions

(1) Superplastic data are now available for several quaternary, quinary and senary HEAs with tensile

elongations up to >1000% under strain rates of the order of $\sim 10^{-2}\,s^{-1}$. The well-known CoCrFeNiMn HEA revealed the maximum total elongation up to 600% after HPT processing followed by tensile pulling at 700°C. The minor addition of Ti or Al to the CoCrFeNiMn HEA led to a significant increase in the maximum total elongations up to 600% and 2000%, respectively.

(2) Grain boundary sliding appears at high temperatures and low strain rates in severely deformed HEAs with the fine and ultrafine grain sizes responsible for the occurrence of superplasticity in the HEAs which is similar to conventional materials despite the sluggish diffusion in this new class of material.

(3) The decomposition of severely deformed single-phase HEAs at elevated temperatures and the formation of different precipitates including B2 (NiAl-rich) and sigma (Cr-rich) phases provide a potential for achieving superior superplastic elongations in HEAs by restricting the grain growth in these alloys during tensile testing.

(4) An analysis of the experimental data and a systematic comparison with conventional superplastic materials show good agreement between the measured strain rates and the theoretical predictions for conventional alloys and superplastic HEAs processed by severe plastic deformation.

Acknowledgements

This study was supported in part by the National Science Foundation of the United States under Grant No. CMMI-2051205 (MK) and by the European Research Council under ERC Grant Agreement No. 267464-SPDMETALS (TGL).

REFERENCES

1) J.W. Yeh, S.K. Chen, S.J. Lin, J.Y. Gan, T.S. Chin, T.T. Shun, C.H. Tsau and S.Y. Chang: Adv. Eng. Mater. **6** (2004) 299–303.
2) B. Cantor, I.T.H. Chang, P. Knight and A.J.B. Vincent: Mater. Sci. Eng. A **375–377** (2004) 213–218.
3) P.K. Huang, J.W. Yeh, T.T. Shun and S.K. Chen: Adv. Eng. Mater. **6** (2004) 74–78.
4) C.-J. Tong, Y.-L. Chen, J.-W. Yeh, S.-J. Lin, S.-K. Chen, T.-T. Shun, C.-H. Tsau and S.-Y. Chang: Metall. Mater. Trans. A **36** (2005) 881–893.
5) U.S. Hsu, U.D. Hung, J.W. Yeh, S.K. Chen, Y.S. Huang and C.C. Yang: Mater. Sci. Eng. A **460–461** (2007) 403–408.
6) J.W. Yeh: Ann. Chim. Sci. Mat. **31** (2006) 633–648.
7) M.H. Tsai and J.W. Yeh: Mater. Res. Lett. **2** (2014) 107–123.
8) D.B. Miracle and O.N. Senkov: Acta Mater. **122** (2017) 448–511.
9) Z. Li, S. Zhao, R.O. Ritchie and M.A. Meyers: Prog. Mater. Sci. **102** (2019) 296–345.
10) H. Inui, K. Kishida and Z. Chen: Mater. Trans. **63** (2022) 394–401.
11) T.-T. Shun, C.-Y. Hsieh, W.-J. Hung and C.-F. Lee: Mater. Trans. **59** (2018) 730–733.
12) M.S. Mehranpour, H. Shahmir and H.S. Kim: J. Alloy. Compd. **944** (2023) 169207.
13) H. Shahmir, M.S. Mehranpour, S.A.A. Shams and T.G. Langdon: J. Mater. Res. Tech. **23** (2023) 3362–3423.
14) B. Schuh, F. Mendez-Martin, B. Völker, E.P. George, H. Clemens, R. Pippan and A. Hohenwarter: Acta Mater. **96** (2015) 258–268.
15) M.J. Zehetbauer and Y.T. Zhu: *Bulk Nanostructured Materials*, (Wiley-Vch Verlag GmbH & Co., 2009) pp. 21–47.
16) P. Asghari-Rad, P. Sathiyamoorthi, N.T.-C. Nguyen, A. Zargaran, T.S. Kim and H.S. Kim: Scr. Mater. **190** (2021) 69–74.
17) H. Shahmir, M. Nili-Ahmadabadi, Y. Huang, J.M. Jung, H.S. Kim and T.G. Langdon: Mater. Sci. Eng. A **626** (2015) 203–206.
18) K. Edalati, E. Akiba and Z. Horita: Sci. Technol. Adv. Mater. **19** (2018) 185–193.
19) K. Edalati *et al.*: Mater. Res. Lett. **10** (2022) 163–256.
20) W. Skrotzki, A. Pukenas, E. Odor, B. Joni, T. Ungar, B. Völker, A. Hohenwarter, R. Pippan and E.P. George: Crystals **10** (2020) 336.
21) H. Shahmir, P. Asghari-Rad, M.S. Mehranpour, F. Forghani, H.S. Kim and M. Nili-Ahmadabadi: Mater. Sci. Eng. A **807** (2021) 140875.
22) K.-Y. Tsai, M.-H. Tsai and J.-W. Yeh: Acta Mater. **61** (2013) 4887–4897.
23) M.S. Mehranpour, H. Shahmir and M. Nili-Ahmadabadi: Mater. Lett. **288** (2021) 129359.
24) T. Chou, J. Huang, C. Yang, S. Lin and T. Nieh: Acta Mater. **195** (2020) 71–80.
25) H. Shahmir, M. Kawasaki and T.G. Langdon: IOP Conf. Ser. Mater. Sci. Eng. **194** (2017) 012040.
26) T.G. Langdon: J. Mater. Sci. **44** (2009) 5998–6010.
27) A.J. Barnes: J. Mater. Eng. Perform. **16** (2007) 440–454.
28) T.G. Langdon: Metall. Trans. A **13** (1982) 689–701.
29) R.Z. Valiev, R.K. Islamgaliev and I.V. Alexandrov: Prog. Mater. Sci. **45** (2000) 103–189.
30) R.Z. Valiev, Y. Estrin, Z. Horita, T.G. Langdon, M.J. Zechetbauer and Y.T. Zhu: JOM **58**(4) (2006) 33–39.
31) Y. Estrin and A. Vinogradov: Acta Mater. **61** (2013) 782–817.
32) T.G. Langdon: Acta Mater. **61** (2013) 7035–7059.
33) R.Z. Valiev, Y. Estrin, Z. Horita, T.G. Langdon, M.J. Zehetbauer and Y. Zhu: JOM **68** (2016) 1216–1226.
34) R.Z. Valiev, O.A. Kaibyshev, R.I. Kuznetsov, R.Sh. Musalimov and N.K. Tsenev: Dokl. Akad. Nauk SSSR **301** (1988) 864–866.
35) T.G. Langdon: Solid State Phenomena **306** (2020) 1–8.
36) R.Z. Valiev and T.G. Langdon: Prog. Mater. Sci. **51** (2006) 881–981.
37) A.P. Zhilyaev and T.G. Langdon: Prog. Mater. Sci. **53** (2008) 893–979.
38) R. Motallebi, Z. Savaedi and H. Mirzadeh: Arch. Civ. Mech. Eng. **22** (2022) 20.
39) T.G. Langdon: Mater. Sci. Eng. A **174** (1994) 225–230.
40) L.K.L. Falk, P.R. Howell, G.L. Dunlop and T.G. Langdon: Acta Metall. **34** (1986) 1203–1214.
41) R.Z. Valiev and T.G. Langdon: Acta Metall. Mater. **41** (1993) 949–954.
42) T.G. Langdon: Acta Metall. Mater. **42** (1994) 2437–2443.
43) J. Wongsa-Ngam, M. Kawasaki and T.G. Langdon: J. Mater. Sci. **48** (2013) 4653–4660.
44) R.B. Figueiredo and T.G. Langdon: J. Mater. Res. Technol. **14** (2021) 137–159.
45) M. Kawasaki and T.G. Langdon: J. Mater. Sci. **42** (2007) 1782–1796.
46) M. Kawasaki and T.G. Langdon: J. Mater. Sci. **49** (2014) 6487–6496.
47) M. Kawasaki and T.G. Langdon: J. Mater. Sci. **51** (2016) 19–32.
48) B.S. Murty, J.W. Yeh and S. Ranganathan: *High-entropy Alloys*, (Elsevier, 2014).
49) O. Ivasishin, S. Shevchenko and S. Semiatin: Mater. Sci. Eng. A **332** (2002) 343–350.
50) Z. Huda and T. Zaharinie: J. Alloy. Compd. **478** (2009) 128–132.
51) J.J. Bhattacharyya, S. Agnew and G. Muralidharan: Acta Mater. **86** (2015) 80–94.
52) G. Azizi, H. Mirzadeh and M. Habibi Parsa: Steel Res. Int. **87** (2016) 820–823.
53) H. Shahmir, M.S. Mehranpour, S.A.A. Shams, C.S. Lee and T.G. Langdon: High Entropy Alloys & Materials **1** (2022) 1–12.
54) X.-M. Chen, Y. Lin and F. Wu: J. Alloy. Compd. **724** (2017) 198–207.
55) W. Liu, Y. Wu, J. He, T. Nieh and Z. Lu: Scr. Mater. **68** (2013) 526–529.
56) J. He, C. Zhu, D. Zhou, W. Liu, T. Nieh and Z. Lu: Intermetallics **55** (2014) 9–14.
57) Y.B. Kang, S.H. Shim, K.H. Lee and S.I. Hong: Mater. Res. Lett. **6** (2018) 689–695.
58) Y.-K. Kim, S. Yang and K.-A. Lee: Addit. Manuf. **36** (2020) 101543.
59) J.Y. Ko and S.I. Hong: J. Alloy. Compd. **743** (2018) 115–125.
60) D.E. Jodi, J. Park, B. Straumal and N. Park: Mater. Lett. **258** (2020) 126806.
61) J. Peng, Z. Li, L. Fu, X. Ji, Z. Pang and A. Shan: J. Alloy. Compd. **803**

(2019) 491–498.
62) H. Khodashenas and H. Mirzadeh: J. Mater. Res. Tech. **21** (2022) 3795–3814.
63) M.R. Zamani, H. Mirzadeh, M. Malekan, S.C. Cao and J.-W. Yeh: High Entropy Alloys & Materials **1** (2022) 1–35.
64) D. Shaysultanov, N. Stepanov, A. Kuznetsov, G. Salishchev and O. Senkov: JOM **65** (2013) 1815–1828.
65) A.V. Kuznetsov, D.G. Shaysultanov, N.D. Stepanov, G.A. Salishchev and O.N. Senkov: Mater. Sci. Eng. A **533** (2012) 107–118.
66) N. Stepanov, D. Shaysultanov, G.A. Salishchev and O. Senkov: Mater. Sci. Forum **838–839** (2016) 302–307.
67) S.R. Reddy, S. Bapari, P.P. Bhattacharjee and A.H. Chokshi: Mater. Res. Lett. **5** (2017) 408–414.
68) H. Shahmir, J. He, Z. Lu, M. Kawasaki and T.G. Langdon: Mater. Sci. Eng. A **685** (2017) 342–348.
69) R.Z. Valiev, B. Straumal and T.G. Langdon: Annu. Rev. Mater. Res. **52** (2022) 357–382.
70) R. Valiev: Nat. Mater. **3** (2004) 511–516.
71) M.S. Mehranpour, H. Shahmir, P. Asghari-Rad, M. Hosseinzadeh, N. Rasooli, H.S. Kim and M. Nili-Ahmadabadi: Materialia **22** (2022) 101394.
72) M.S. Mehranpour, H. Shahmir, A. Derakhshandeh and M. Nili-Ahmadabadi: J. Alloy. Compd. **888** (2021) 161530.
73) M.S. Mehranpour, H. Shahmir and M. Nili-Ahmadabadi: J. Alloy. Compd. **840** (2020) 155672.
74) M.S. Mehranpour, H. Shahmir and M. Nili-Ahmadabadi: Mater. Sci. Eng. A **793** (2020) 139884.
75) H. Shahmir, J. He, Z. Lu, M. Kawasaki and T.G. Langdon: Mater. Sci. Eng. A **676** (2016) 294–303.
76) H. Shahmir, T. Mousavi, J. He, Z. Lu, M. Kawasaki and T.G. Langdon: Mater. Sci. Eng. A **705** (2017) 411–419.
77) H. Shahmir, M. Nili-Ahmadabadi, A. Shafiee and T.G. Langdon: Mater. Sci. Eng. A **718** (2018) 468–476.
78) N.T.-C. Nguyen, P. Asghari-Rad, P. Sathiyamoorthi, A. Zargaran, C.S. Lee and H.S. Kim: Nat. Commun. **11** (2020) 2736.
79) H. Jeong and W.J. Kim: J. Alloy. Compd. **869** (2021) 159256.
80) N.T.-C. Nguyen, P. Asghari-Rad, H. Park and H.S. Kim: J. Mater. Sci. **57** (2022) 18154–18167.
81) H. Shahmir, M.S. Mehranpour, A. Derakhshandeh and M. Nili-Ahmadabadi: Mater. Charact. **182** (2021) 111513.
82) N.T.-C. Nguyen, J. Moon, P. Sathiyamoorthi, P. Asghari-Rad, G.H. Kim, C.S. Lee and H.S. Kim: Mater. Sci. Eng. A **764** (2019) 138198.
83) S. Nene, K. Liu, S. Sinha, M. Frank, S. Williams and R. Mishra: Materialia **9** (2020) 100521.
84) N.T.-C. Nguyen, P. Asghari-Rad, J.W. Bae, P. Sathiyamoorthi and H.S. Kim: Metall. Mater. Trans. A **52** (2021) 1–7.
85) P. Asghari-Rad, N.T.-C. Nguyen, A. Zargaran, P. Sathiyamoorthi and H.S. Kim: Scr. Mater. **207** (2022) 114239.
86) N.T.-C. Nguyen, P. Asghari-Rad, A. Zargaran, E.S. Kim, P. Sathiyamoorthi and H.S. Kim: Scr. Mater. **221** (2022) 114949.
87) T.G. Langdon: Met. Sci. **16** (1982) 175–183.
88) F.A. Mohamed and T.G. Langdon: Acta Metall. **22** (1974) 779–788.
89) G. Laplanche, P. Gadaud, O. Horst, F. Otto, G. Eggeler and E. George: J. Alloy. Compd. **623** (2015) 348–353.
90) A.V. Kuznetsov, D.G. Shaisultanov, N. Stepanov, G.A. Salishchev and O.N. Senkov: Mater. Sci. Forum **735** (2013) 146–151.
91) P. Asghari-Rad, P. Sathiyamoorthi, N.T.-C. Nguyen, J.W. Bae, H. Shahmir and H.S. Kim: Mater. Sci. Eng. A **771** (2020) 138604.